

Effect of Alkyltrimethylammonium Ions on Corrosion and Electrochemical Behavior of Pb-Ca-Sn Alloy

Kacper Kopczyński¹, Agnieszka Gabryelczyk¹, Marek Baraniak¹, Bartosz Łęgosz¹,
Juliusz Pernak¹, Paweł Kędzior², Grzegorz Lota^{1,*}

¹ Faculty of Chemical Technology, Poznan University of Technology, Berdychowo 4, 60-965 Poznan, Poland

² PPUH AUTOPART Jacek Bąk Sp. z o.o., Kwiatkowskiego 2a, 39-300 Mielec, Poland

*E-mail: grzegorz.lota@put.poznan.pl

Received: 7 July 2018 / Accepted: 23 August 2018 / Published: 1 October 2018

Due to the increasing competition on the chemical power sources market, lead-acid batteries must improve their parameters and functionality. A modification of electrolyte composition is suggested in the presented paper for better corrosion inhibition and enhancement of the stability of the sulfuric acid-based electrolyte during charging process. Ten quaternary ammonium-based ionic liquids have been employed as additives to electrolyte. The differences between used compounds have been based on different types of anion in the molecule (sulfate and bisulfate) and the length of the substituent incorporated in the cation. The electrochemical window of the electrolyte in terms of onset potentials of hydrogen and oxygen evolution reactions, corrosion potential, corrosion current density and polarization resistance of the alloy in case of corrosion have been the parameters evaluated based on the undertaken experiments. It has been noted that the length of the side chain in the molecule has a great impact on the final properties of ionic liquids. Experiments have shown that hexadecyltrimethylammonium-based ionic liquids contributed to the most visible improvement in comparison to the other compounds. Significance of the anion in the molecule has been also observed, bisulfate anion appeared to be beneficial for the overall performance of the lead-calcium-tin alloy electrode.

Keywords: Ionic liquids; corrosion; current collector; lead alloy; lead-acid battery

1. INTRODUCTION

Lead-acid battery was invented over 150 years ago by the French physicist Gaston Planté. It exhibits appropriate electrochemical properties and ensures satisfying reliability which makes it a perfect device for SLI (starting, lighting, ignition) battery application. Despite the fact that they are

known for a long time and are successful in the industry as well as on the chemical power sources market, lead-acid batteries possess some disadvantages and can suffer from several major problems. One of the biggest difficulties in case of lead-acid batteries is corrosion of current collectors (grids).

Corrosion of current collectors, next to sulfation of the electrode and softening along with shedding of the positive active mass, is the most common cause of the lead-acid batteries failure [1,2]. This makes corrosion of lead-acid battery current collectors a research topic which cannot be ignored in following years by researchers as well as by manufacturers. Observation of the anodic excursion peak is among new methods of measuring the corrosion rate [3,4].

One of the methods to reduce the corrosion rate in lead-acid batteries is to alloy the lead with other metals to improve the corrosion resistance of the grid. Many types of new alloys were tested in terms of improvement of that specific property, e.g. tin [5], silver [6,7], bismuth [7,8] or even rare earth metals [9-13]. This approach yields very good results, furthermore, its impact on the technology is acceptable and limited mostly to melting adequate amounts of needed components and casting of the liquid alloy. However, its use is often limited by the high cost of the required alloying elements. Incorporation of corrosion inhibitors to electrolyte of the lead-acid battery seemed to be less demanding.

Many compounds were tested as potential corrosion inhibitors of lead alloys in sulfuric acid solutions, such as phosphoric acid [14,15], boric acid [15] or several amino acids [16,17]. Ionic liquids are a new type of compounds which gathered scientific attention in a variety of fields. Ionic liquids found many applications in modern chemistry due to their exceptional properties such as being designer solvents, good thermal and electrochemical stability and negligible vapour pressure [18]. They can be also used in lead-acid battery application [19-22]. They extend the electrochemical stability of electrolyte, hinder the corrosion of lead alloys and increase the discharge capacity of lead-acid cells.

In this study, the influence of bisulfate and sulfate quaternary ammonium salts on corrosion of lead-calcium-tin alloy was presented. The mentioned Pb-Ca-Sn alloy is used during large scale production of the current collectors in lead-acid batteries. The purpose of the presented work was to correlate the length of the substituent and the type of anion in the molecule with the influence of the used compound on the stability of the electrolyte for lead-acid battery and the corrosion intensity of the lead alloy.

2. EXPERIMENTAL

2.1. Synthesis of ionic liquids

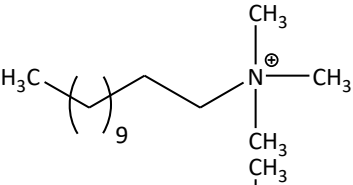
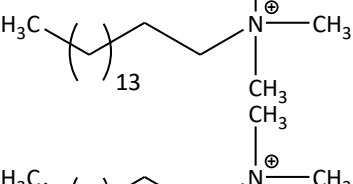
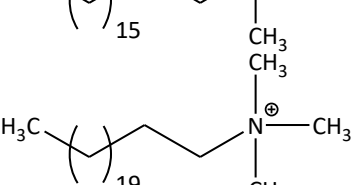
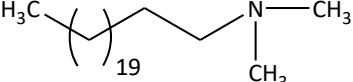
Materials used for the synthesis of specific ionic liquids were: sulfuric acid (98%), hexyltrimethylammonium bromide (min. 98%), dodecyltrimethylammonium (min. 98%), hexadecyltrimethylammonium (min. 98%), trimethyloctadecylammonium (min. 95%) and docosyltrimethylammonium (90%) chlorides, which were acquired from Merck. Potassium hydroxide (min. 99%) and all solvents (methanol, 2-propanol, DMSO, acetonitrile, acetone, ethyl acetate,

chloroform, toluene and hexane) were delivered by Avantor Performance Materials. All chemicals were used as obtained, without purifying.

The syntheses were performed as follows: 0.01 mol of quaternary chloride was dissolved in 30 mL of 2-propanol and then 0.01 mol of potassium hydroxide in 2-propanol was added. The reagents were mixed for 15 minutes. The precipitated inorganic salt was filtered off and stoichiometric amount of concentrated sulfuric acid was slowly added to the solution containing 0.005 mol of the quaternary hydroxide to obtain specific sulfates and 0.01 mol to obtain quaternary bisulfates. The solvent and water formed as by-products were then evaporated and the products were dried under vacuum at 60 °C. The structural formulas of the synthesized ionic liquids with their abbreviations used in the text were showed in Table 1.

Table 1. List of ionic liquids with their structural formulas and abbreviations.

No.	Chemical name	Structural formula	Abbreviation
1	Di(hexyltrimethylammonium) sulfate		C6SO4
2	Di(dodecyltrimethylammonium) sulfate		C12SO4
3	Di(hexadecyltrimethylammonium) sulfate		C16SO4
4	Di(octadecyltrimethylammonium) sulfate		C18SO4
5	Di(docosyltrimethylammonium) sulfate		C22SO4
6	Hexyltrimethylammonium bisulfate		C6HSO4

7	Dodecyltrimethylammonium bisulfate		HSO_4^-	C12HSO4
8	Hexadecyltrimethylammonium bisulfate		HSO_4^-	C16HSO4
9	Trimethyloctadecylammonium bisulfate		HSO_4^-	C18HSO4
10	Docosyltrimethylammonium bisulfate		HSO_4^-	C22HSO4

2.2. Elemental analysis and NMR spectroscopy of ionic liquids

^1H NMR spectra were acquired by Varian Mercury 300 spectrometer operating at 300 MHz with tetramethyl silane (TMS) as the internal standard. ^{13}C NMR spectra were obtained using the same instrument at 75 MHz.

2.3. Thermal analysis

Thermal transition temperatures were determined by differential scanning calorimetry (DSC), with a Mettler Toledo Star DSC1 (Leicester, UK) unit, under nitrogen. ILs (between 5 and 15 mg) were placed in aluminium pans and heated from 25 to 120 °C at a heating rate of 10 °C min⁻¹, cooled afterwards with an intracooler at a cooling rate of 10 °C min⁻¹ to -100 °C, then heated again to 120 °C. Thermogravimetric analysis was performed using a Mettler Toledo STARE TGA/DSC1 (Leicester, UK), under nitrogen. ILs (between 2 and 10 mg) were placed in aluminium pans and heated from 30 to 450 °C at a heating rate of 10 °C min⁻¹.

2.4. Elemental ICP analysis

Elemental ICP analysis of lead-calcium-tin alloy was performed using AGILENT 725 ES ICP Optical Emission Spectrometer.

2.5. Electrochemical examination

All electrochemical measurements were performed in the 3-electrode set-up in the cylindrical vessel, where lead-calcium-tin alloy was used as a working electrode, counter electrode was made of

lead (99%) and reference electrode was mercury/mercurous sulfate in 1M sulfuric acid ($\text{Hg}|\text{Hg}_2\text{SO}_4$ in 1M H_2SO_4). To release gaseous products from the electrochemical cell, ventilation holes were located in the top lid of the vessel. Working and counter electrode materials were supplied by AutoPart Company (Mielec, Poland) in the form of wide straps, prepared for further processing by expanded metal method. The working electrode was disk-shaped with the surface area equal to 4.5 cm^2 . The surface area of the counter electrode was two times greater to provide effective charge transfer. Before each experiment, the surfaces of the working and counter electrodes were mechanically polished with wet sandpaper grade P2500. The electrolyte for electrochemical measurements was 37 wt.% sulfuric acid solution prepared by dilution of 98 wt.% H_2SO_4 (Merck) with distilled water with addition of 5 mg cm^{-3} of the respective ionic liquid. Reference electrolyte, without ILs, was also tested to analyse the initial corrosion parameters of used Pb-Ca-Sn alloy.

Electrochemical stability of the electrolyte was studied using linear sweep voltammetry technique (LSV) at a scan rate of 10 mV s^{-1} .

Corrosion measurements of the alloy in all of the electrolytes were a combination of electrochemical impedance spectroscopy (EIS) and linear sweep voltammetry (LSV). EIS was carried out within a frequency range from 50 mHz to 10 kHz at open circuit voltage (OCV) with amplitude 7 mV RMS. The LSV measurements were conducted at a scan rate equal to 0.2 mV s^{-1} , with potential range from -180 mV to $+180\text{ mV}$ versus open circuit voltage. The corrosion measurements were conducted after 5 hours at OCV to ensure stable conditions.

Electrochemical experiments were performed under ambient conditions using the multichannel potentiostat/galvanostat VMP3 BioLogic® (France) with EC-Lab® software and repeated at least three times. The numbers presented in the table are average values of calculated parameters.

3. RESULTS AND DISCUSSION

3.1. Elemental analysis and NMR spectroscopy results

Di(hexyltrimethylammonium) sulfate (C_6SO_4)

^1H NMR (300 MHz, MeOH-d_4): 0.91–0.95 (t, 6H); 1.36–1.40 (m, 12H); 1.75–1.82 (m, 4H); 3.16 (s, 18H); 3.33–3.37 (m, 4H).

^{13}C NMR (75 Hz, MeOH-d_4): 14.4; 23.5; 23.9; 27.0; 32.5; 53.6; 67.8.

Elem. Anal. CHN for $\text{C}_{18}\text{H}_{44}\text{N}_2\text{O}_4\text{S}$ ($M = 384.62\text{ g mol}^{-3}$): calcd.: C = 56.21; H = 11.53; N = 7.28; found: C = 56.53; H = 11.74; N = 7.31.

Di(dodecyltrimethylammonium) sulfate (C_{12}SO_4)

^1H NMR (300 MHz, CDCl_3): 0.86–0.91 (t, 6H), 1.19–1.31 (m, 36H); 1.66 (m, 4H); 3.33 (s, 18H); 3.38–3.41 (m, 4H).

^{13}C NMR (75 Hz, CDCl_3): 13.9; 22.5; 23.0; 26.2; 29.2; 29.3; 29.4; 29.5; 31.8; 52.9; 66.1.

Elem. Anal. CHN for $C_{30}H_{68}N_2O_4S$ ($M = 552.94 \text{ g mol}^{-3}$): calcd.: C = 65.16; H = 12.40; N = 5.07; found: C = 64.90; H = 12.07; N = 4.89.

Di(hexadecyltrimethylammonium) sulfate ($C_{16}SO_4$)

1H NMR (300 MHz, $CDCl_3$): 0.86–0.90 (t, 6H); 1.25–1.31 (m, 52H); 1.67 (m, 4H); 3.46 (s, 18H); 3.48–3.52 (m, 4H).

^{13}C NMR (75 Hz, $CDCl_3$): 13.8; 22.4; 23.0; 26.0; 29.1; 29.2; 29.3; 29.4; 31.6; 52.6; 66.1.

Elem. Anal. CHN for $C_{38}H_{84}N_2O_4S$ ($M = 665.15 \text{ g mol}^{-3}$): calcd.: C = 68.62; H = 12.73; N = 4.21; found: C = 68.91; H = 13.00; N = 4.45.

Di(octadecyltrimethylammonium) sulfate ($C_{18}SO_4$)

1H NMR (300 MHz, $CDCl_3$): 0.79–0.83 (t, 6H); 1.09–1.25 (m, 60H); 1.60 (m, 4H); 3.34 (s, 18H); 3.36–3.40 (m, 4H).

^{13}C NMR (75 Hz, $CDCl_3$): 13.9; 22.5; 23.0; 26.2; 29.2; 29.3; 29.4; 29.5; 29.6; 31.7; 52.8; 66.2.

Elem. Anal. CHN for $C_{42}H_{92}N_2O_4S$ ($M = 721.26 \text{ g mol}^{-3}$): calcd.: C = 69.94; H = 12.86; N = 3.88; found: C = 70.15; H = 13.10; N = 4.12.

Di(docosyltrimethylammonium) sulfate ($C_{22}SO_4$)

1H NMR (300 MHz, $CDCl_3$): 0.86–0.90 (t, 6H); 1.26–1.32 (m, 76H); 1.69 (m, 4H); 3.39 (s, 18H); 3.41–3.45 (m, 4H).

^{13}C NMR (75 Hz, $CDCl_3$): 14.0; 22.6; 23.1; 26.2; 29.3; 29.4; 29.5; 29.6; 29.7; 31.8; 53.0; 66.5.

Elem. Anal. CHN for $C_{50}H_{108}N_2O_4S$ ($M = 833.47 \text{ g mol}^{-3}$): calcd.: C = 72.05; H = 13.06; N = 3.36; found: C = 71.83; H = 12.89; N = 3.01.

Hexyltrimethylammonium bisulfate (C_6HSO_4)

1H NMR (300 MHz, $MeOH-d_4$): 0.91–0.94 (t, 3H); 1.36–1.41 (m, 6H); 1.78 (m, 2H); 3.15 (s, 9H); 3.34–3.38 (m, 2H).

^{13}C NMR (75 Hz, $MeOH-d_4$): 14.3; 23.5; 23.9; 27.0; 32.4; 53.6; 67.8.

Elem. Anal. CHN for $C_9H_{23}NO_4S$ ($M = 241.35 \text{ g mol}^{-3}$): calcd.: C = 44.79; H = 9.61; N = 5.80; found: C = 44.44; H = 9.26; N = 5.48.

Dodecyltrimethylammonium bisulfate ($C_{12}HSO_4$)

1H NMR (300 MHz, $CDCl_3$): 0.86–0.90 (t, 3H); 1.19–1.32 (m, 18H); 1.70 (m, 2H); 3.26 (s, 9H); 3.36–3.41 (m, 2H).

^{13}C NMR (75 Hz, $CDCl_3$): 13.8; 22.4; 22.9; 26.0; 29.1; 29.4; 29.5; 31.7; 52.7; 66.3.

Elem. Anal. CHN for $C_{15}H_{35}NO_4S$ ($M = 325.51 \text{ g mol}^{-3}$): calcd.: C = 55.35; H = 10.84; N = 4.30; found: C = 55.59; H = 11.00; N = 4.61.

Hexadecyltrimethylammonium bisulfate ($C_{16}HSO_4$)

1H NMR (300 MHz, $CDCl_3$): 0.86–0.90 (t, 3H); 1.18–1.32 (m, 26H); 1.70 (m, 2H); 3.28 (s, 9H); 3.36–3.42 (m, 2H).

^{13}C NMR (75 Hz, CDCl_3): 14.0; 22.6; 23.1; 26.2; 29.3; 29.5; 29.6; 29.7; 31.8; 52.9; 66.4.

Elem. Anal. CHN for $\text{C}_{19}\text{H}_{43}\text{NO}_4\text{S}$ ($M = 381.61 \text{ g mol}^{-3}$): calcd.: C = 59.80; H = 11.36; N = 3.67; found: C = 60.14; H = 11.54; N = 3.87.

Trimethyloctadecylammonium bisulfate ($\text{C}_{18}\text{HSO}_4$)

^1H NMR (300 MHz, $\text{MeOH}-d_4$): 0.87–0.92 (t, 3H); 1.22–1.40 (m, 30H); 1.78 (m, 2H); 3.12 (s, 9H); 3.31–3.35 (m, 2H).

^{13}C NMR (75 Hz, $\text{MeOH}-d_4$): 14.5; 23.8; 24.0; 27.4; 30.3; 30.5; 30.6; 30.7; 30.8; 33.11; 53.6; 67.9.

Elem. Anal. CHN for $\text{C}_{21}\text{H}_{47}\text{NO}_4\text{S}$ ($M = 409.67 \text{ g mol}^{-3}$): calcd.: C = 61.57; H = 11.56; N = 3.42; found: C = 61.92; H = 11.88; N = 3.61.

Docosyltrimethylammonium bisulfate ($\text{C}_{22}\text{HSO}_4$)

^1H NMR (300 MHz, $\text{MeOH}-d_4$): 0.86–0.90 (t, 3H); 1.27–1.38 (m, 38H); 1.76 (m, 2H); 3.11 (s, 9H); 3.29–3.34 (m, 2H).

^{13}C NMR (75 Hz, $\text{MeOH}-d_4$): 14.5; 23.8; 24.0; 27.4; 30.3; 30.5; 30.6; 30.7; 30.8; 30.9; 33.1; 53.5; 67.9.

Elem. Anal. CHN for $\text{C}_{25}\text{H}_{55}\text{NO}_4\text{S}$ ($M = 465.77 \text{ g mol}^{-3}$): calcd.: C = 64.47; H = 11.90; N = 3.01; found: C = 64.15; H = 11.74; N = 3.20.

The structures of the obtained compounds were confirmed by analysis of NMR spectra. The values of chemical shifts recorded with use of different solvents (chloroform or methanol) were slightly different.

Protons in methyl groups of the alkyl substituents generated signals in the ranges of 0.79–0.91 ppm for chloroform and 0.86–0.95 when methanol was used. Methylene groups occurred at signals between 1.09 and 1.32 ppm for chloroform and between 1.22 and 1.41 ppm for methanol. Protons of methylene groups in position B to quaternary nitrogen atom were identified as signals between 1.60 and 1.70 ppm for chloroform and between 1.70 and 1.82 ppm for methanol. Protons in methyl groups bonded directly with the quaternary nitrogen atom generated strong signals in ranges 3.26–3.46 ppm for chloroform and 3.11–3.16 ppm for methanol. The methylene groups in position A to the nitrogen atom were observed in ranges 3.36–3.52 ppm and 3.29–3.38 ppm for chloroform and methanol, respectively.

3.2. Thermal analysis results

Transition temperatures of the synthesized compounds were presented in Table 2. Among the synthesized sulfates only IL with the shortest aliphatic substituent (C_6SO_4) exhibited glass transition, which was observed at -2.47°C . Di(dodecyltrimethylammonium) sulfate (C_{12}SO_4) showed multiple signals between -16.28 and 73.35°C for crystallization, and between -8.37 and 88.48°C for melting. Similar observations were made in case of the di(octadecyltrimethylammonium) ionic liquid

(C18SO₄), as a broad signal between 58.22 and 102.19 °C was noted for melting. It can be explained by multiple polymorphic solid-solid transitions, which were observed for ILs with long alkyl substituents [23]. The observed transitions temperatures increased with the elongation of the alkyl substituent.

For the synthesized bisulfates glass transition temperatures were observed in the range from −39.55 to 61.91 °C. No glass transition was detected for C18HSO₄. The crystallization temperatures varied from 7.15 (C6HSO₄) to 80.43 °C (C22HSO₄) and increased with elongation of the alkyl chain. Double melting transition occurred for C18HSO₄, at 65.04 and 72.39 °C and can be explained by thermal memory of the sample. Other bisulfates melted in range from 44.08 (C6HSO₄) to 90.02 °C (C16HSO₄).

Generally, the obtained bisulfates were more thermally stable than sulfates. The lowest temperature resulting in 5% loss of the sample was observed at 187 °C for sulfate C6SO₄ and at 242 °C for bisulfate C22HSO₄.

Table 2. Thermal analysis results.

Sample IL	T _g ^a	T _c ^b	T _m ^c	T _{onset5%} ^d	T _{onset50%} ^e
			[°C]		
C6SO₄	−2.47	3.85	6.61	187	272
	—	−16.28; 15.56;	−8.37; 20.69;	205	296
C12SO₄		35.94; 64.22;	32.82; 47.81;		
		73.35	88.48		
C16SO₄	—	51.93	45.86	199	297
C18SO₄	—	65.93	58.22–102.19	203	292
C22SO₄	—	83.87	73.86	208	251
C6HSO₄	−39.55	7.15	44.08	258	324
C12HSO₄	−27.82	46.31	56.44	258	311
C16HSO₄	61.91	78.61	90.02	279	315
C18HSO₄	—	65.43	65.04; 72.39	280	316
C22HSO₄	13.54	80.43	81.15	242	310

^aglass transition, ^bcrystallization temperature, ^cmelting point, ^dtemperature value which results in 5% mass loss, ^etemperature value which results in 50% mass loss

3.3 ICP

Composition of the used lead-calcium-tin alloy was as follows: 98.928 wt.% of Pb, 0.073 wt.% of Ca, 0.976 wt.% of Sn, other elements comprised 0.023 wt.% of the sample. The presented values confirmed that the material for current collectors comprises the standard of a lead-based alloy for the use in the automotive industry.

3.4. Electrochemical study

The study of the electrochemical stability of electrolytes with and without bisulfate ionic liquids (Fig. 1) revealed that changes in oxygen evolution reaction (OER) potential were negligible. In

all the cases, the shift did not exceed 10 mV. On the other hand, great differences can be observed for the hydrogen evolution reaction (HER) potentials. With increasing length of side chain in order C6HSO₄, C12HSO₄, C16HSO₄, there is a shift to more negative values of the HER potential by 50 mV, 152 mV and 176 mV, respectively. With further increase of side chain length, changes in the HER potential were smaller and reached 118 mV for C18HSO₄ and 96 mV for C22HSO₄. Addition of the best studied bisulfate ionic liquid, C16HSO₄, allowed to extend the electrochemical window by 186 mV in total. In all cases peaks from oxidation of lead to lead sulfate and reduction of lead sulfate to lead near potential equal to -1.0 V (vs. Hg|Hg₂SO₄ in 1M H₂SO₄) were visible. Additionally, there were no other peaks suggesting ionic liquid decomposition.

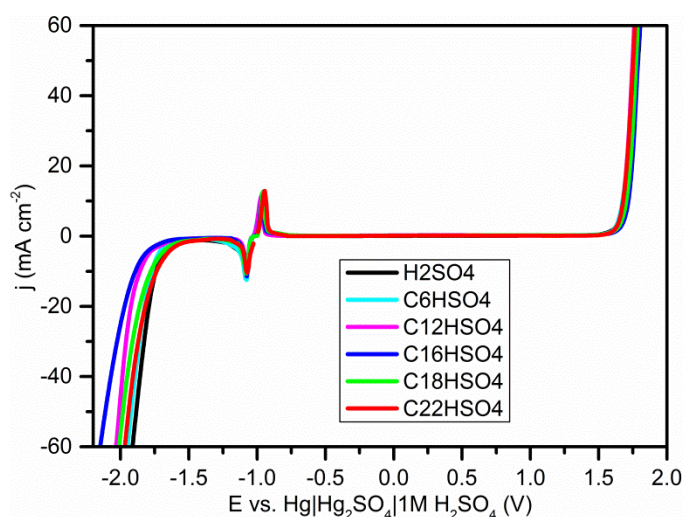


Figure 1. Electrochemical window of the reference electrolyte and electrolytes modified by bisulfate ionic liquids, using linear sweep voltammetry at scan rate 10 mV s^{-1} , potential measured vs. Hg|Hg₂SO₄ reference electrode.

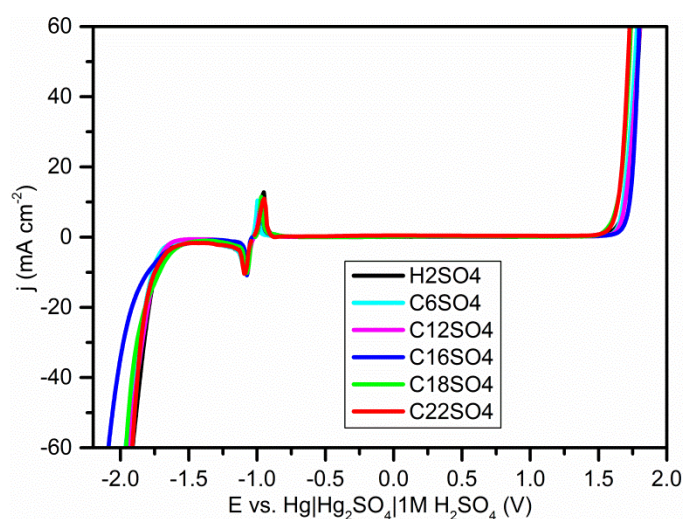


Figure 2. Electrochemical window of the reference electrolyte and electrolytes modified by sulfate ionic liquids, using linear sweep voltammetry at scan rate 10 mV s^{-1} , potential measured vs. Hg|Hg₂SO₄ reference electrode.

The results referring to the stability of electrolytes containing a small addition of ionic liquids with the sulfate anion (Fig. 2), depict similar dependencies in case of HER as that of ILs with the bisulfate anion. This type of ionic liquids had a greater impact on the oxygen evolution reaction potentials. Only electrolyte marked C16SO₄ had higher oxygen evolution reaction potential than the electrolyte without any additions. Potential of this reaction was changed by 22 mV. Electrolytes with the addition of C6SO₄, C12SO₄, C18SO₄ and C22SO₄ had a less positive OER potential than the reference electrolyte by 39 mV, 21 mV, 75 mV and 63 mV, respectively. Hydrogen evolution reaction potential of electrolytes with sulfate ionic liquids was shifted to more negative values in a manner similar to bisulfate ionic liquids. The highest shift was observed for C16SO₄ as an electrolyte addition.

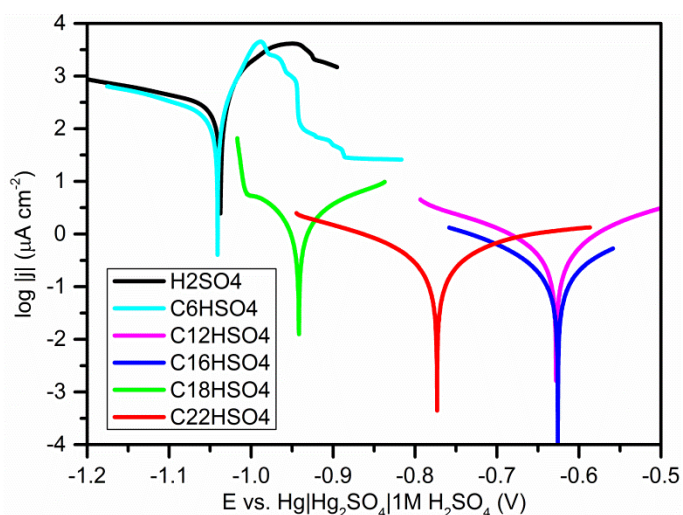


Figure 3. Tafel plots of the examined electrochemical systems containing bisulfate ionic liquids, experiment carried out at a scan rate of 0.2 mV s^{-1} within the potential range of $\pm 180 \text{ mV}$ vs. open circuit potential measured vs. $\text{Hg}|\text{Hg}_2\text{SO}_4$.

Table 3. Corrosion parameters of the electrochemical cell with lead alloy in various electrolytes with bisulfate ionic liquids.

Parameter	Electrolyte					
	Reference solution	C6HSO4	C12HSO4	C16HSO4	C18HSO4	C22HSO4
E_{corr} (Tafel), mV	-1033.4 ± 2.4	-1041.1 ± 0.6	-628.9 ± 0.7	-626.9 ± 0.9	-973.1 ± 0.2	-773.2 ± 0.1
i_{corr} (Tafel), $\mu\text{A cm}^{-2}$	219.3 ± 19.8	135.4 ± 14.5	0.26 ± 0.03	0.20 ± 0.01	0.17 ± 0.01	0.15 ± 0.01
R_p (EIS), $\Omega \text{ cm}^2$	7.9 ± 0.1	97.6 ± 11.9	30222 ± 98	59103 ± 73	10206 ± 54	28165 ± 68
b_a , mV dec ⁻¹	31.5	30.9	125.8	201.1	110.2	100.4
b_c , mV dec ⁻¹	193.6	156	114.7	115.8	93.4	95.6

The HER potential of this compound was changed by 184 mV which resulted in the highest overall increase of the electrochemical stability among all the examined ionic liquids (by 206 mV). For C6SO₄, C12SO₄, C18SO₄ and C22SO₄ additions, the HER potential was shifted by 5 mV, 41 mV, 123 mV and 54 mV, respectively. Similarly to the bisulfate ionic liquid additions, formation of two peaks coming from lead/lead sulfate redox couple was visible around potential -1.0 V (vs. $\text{Hg}|\text{Hg}_2\text{SO}_4$

in 1M H₂SO₄). Also, no other peaks from ionic decomposition can be seen. Tafel plots obtained for the lead-based alloy immersed in the electrolytes which contained bisulfate ionic liquids were presented in Fig. 3. Corrosion parameters of examined systems containing bisulfate ILs were collected in Table 3.

Linear sweep voltammetry measurements showed that in comparison to the reference system, a significant decrease of corrosion current as well as shift of corrosion potential to more positive values of the working electrode can be seen in almost all examined electrolytes with bisulfate ionic liquid addition.

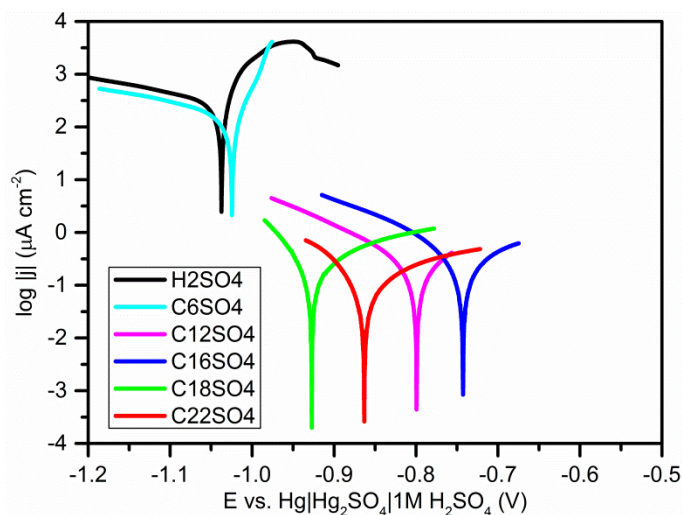


Figure 4. Tafel plots of the examined electrochemical systems containing sulfate ionic liquids, experiment carried out at a scan rate of 0.2 mV s⁻¹ within the potential range of ±180 mV vs. open circuit potential measured vs. Hg|Hg₂SO₄.

Table 4. Corrosion parameters of the electrochemical cell with lead alloy in various electrolytes with sulfate ionic liquids.

Parameter	Electrolyte					
	Reference solution	C6SO ₄	C12SO ₄	C16SO ₄	C18SO ₄	C22SO ₄
E_{corr} (Tafel), mV	-1033.4±2.4	-1024.1±0.5	-799.5±0.8	-742.5±0.4	-931.3±0.8	-862.9±0.3
i_{corr} (Tafel), μA cm ⁻²	219.3±19.8	104.4±23.5	0.11±0.01	0.15±0.01	0.56±0.03	0.05±0.01
R_p (EIS), Ω cm ²	7.9±0.1	15.6±0.7	5017±16	59103±104	4797±26	15412±49
b_a , mV dec ⁻¹	31.5	30.2	117.2	105.8	127.7	125.7
b_c , mV dec ⁻¹	193.6	129.6	107.4	77.2	94.9	60.3

This indicates that a layer of ionic liquid molecules adsorbed on the surface of the alloy. Moreover, this occurrence contributed to the inhibition of the corrosion process of the lead alloy, however, it did not affect the reactions which occur on the electrode. This adsorption was most effective for C16HSO₄, decreasing the corrosion current by approx. 1000 times and moving the corrosion potential by around 400 mV in the direction of the positive values. Used software enabled also to evaluate the values of anodic and cathodic Tafel slopes b_a and b_c . It could be observed, that anodic slopes alloy showed greater values in the electrolytes, where corrosion of the lead-based alloy

was inhibited by the influence of the additive. On the other hand, the values of the cathodic slope decreased along with the corrosion current density.

Linear sweep voltammetry measurements of corrosion process of the PbCaSn working electrode in electrolytes containing sulfate ionic liquids are presented in Fig. 4. Corrosion parameters of examined systems containing sulfate ILs are collected in Table 4.

Similar corrosion inhibition behaviour as in bisulfate ionic liquids was observed. Additionally, for this group of examined compounds an adsorbed layer made of organic particles decreased the corrosion current and shifted the corrosion potential towards more positive values. The highest corrosion intensity was observed, similarly to bisulfate ILs, in the system containing ionic liquid with side chain of sixteen carbon atoms – C16SO₄. In case of this compound, corrosion current decreased by over 1000 times and corrosion potential was shifted by 294 mV to more positive values in the comparison to the reference system. The values of anodic and cathodic Tafel slopes tended to change accordingly to the corrosion behaviour of the electrochemical systems. The value of the anodic slopes tended to rise when corrosion inhibition of the alloy increased, while cathodic slope seemed to decrease when corrosion current density, thus the corrosion rate, was lower.

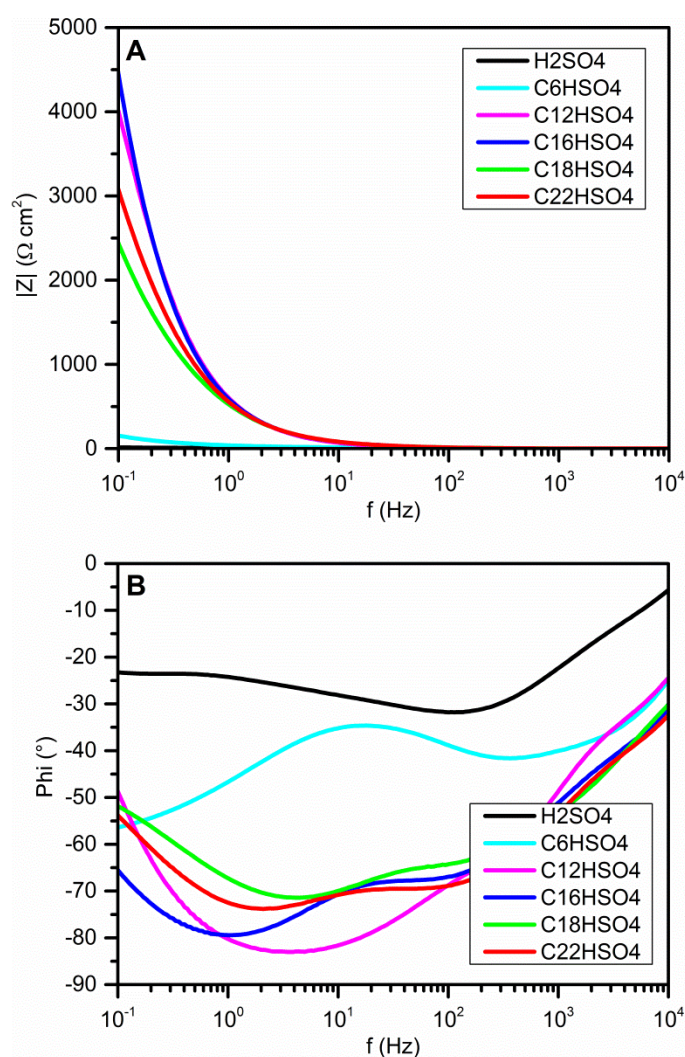


Figure 5. Bode plots of the Pb alloy/modified electrolyte by bisulfate ionic liquids, A) impedance module, B) phase shift.

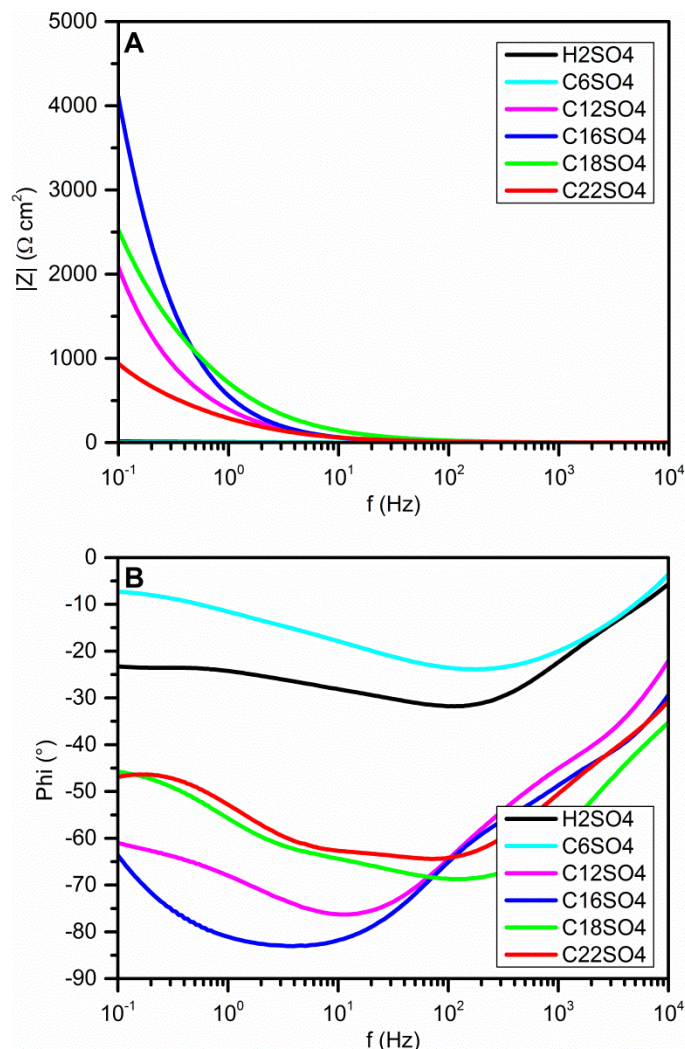


Figure 6. Bode plots of the Pb alloy/modified electrolyte by sulfate ionic liquids, A) impedance module, B) phase shift.

Figure 5 and figure 6 represent Bode plots obtained based on the electrochemical impedance measurements for the lead-calcium-tin alloy immersed in electrolyte containing bisulfate and sulfate ionic liquids, respectively. After five hours in open circuit conditions, the polarization resistance increased. This could be attributed to the appearance of an additional layer which forms on the surface of the electrode. The highest polarization resistance can be observed for electrolytes with additives marked $\text{C}_{16}\text{HSO}_4$ and C_{16}SO_4 . This experiment confirmed the best corrosion inhibition properties of ionic liquids with sixteen carbon atoms in substituent aliphatic chain. First time constant is associated with the charge transfer process, while the second is associated with the diffusion through the freshly formed layer.

The obtained results indicate good anticorrosion properties of the modified electrochemical systems as well as extension of the electrochemical window of the electrolyte with an addition of selected ionic liquids. Similar results concerning the formation of a stable layer on the surface of Pb-Ca-Sb electrode was previously reported for polymeric ionic liquids in sulfuric acid solutions [21,22]. Results reported in this study are more promising. The decrease of corrosion current is similar to the

one obtained for electrolytes with polymeric ionic liquids, nevertheless, the shift of corrosion potential to the more positive values after the addition of C16HSO₄ or C16SO₄ compounds can be observed. The observed effect of shift of hydrogen and oxygen evolution reactions potential on the lead-alloy electrodes was also reported for other bisulfate ionic liquids [24,25]. Moreover, similar effect was observed for ionic liquids with an imidazolium cation as well [20]. Ionic liquids are known for its anticorrosion properties. An addition of 1-ethyl-3-methylimidazolium-based ionic liquids to an acidic electrolyte in amount similar to the proposed one caused the decrease of the oxygen evolution potential on the surface of an lead alloy electrode by 7 to 25 mV. Moreover, it shifted the corrosion potential by only around 30 mV and decreased corrosion current by almost 50% [26].

Application of hexadecyltrimethylammonium-based ionic liquids in presented study made obtained results exceptionally prominent. Some amino acids also exhibit corrosion inhibition properties towards lead alloys for lead-acid battery production [27]. Large increase of polarization resistance was obtained for tryptophane additive which contributed to the decrease of corrosion rate. The highest inhibition efficiency referring to the electrochemical polarization measurements was around 63%. Heteroatoms such as nitrogen in the structure of applied compound significantly increase the inhibition efficiency. Nevertheless, the results obtained by addition of ionic liquids are superior in comparison to amino acids.

Compounds with amphiphilic properties also suppress the corrosion of lead based alloys [28]. Addition of different surfactants to acidic electrolyte reduces corrosion current by 63–72% and similarly to ionic liquids influences the cathodic and anodic Tafel slopes. This kind of compounds also increases the hydrogen and oxygen evolution potentials. Adsorption of long alkyl chains of SDBS or SDS shows good anticorrosion properties. Similar construction has examined ionic liquids. Sodium sulfate added in appropriate concentration to sulfuric acid electrolyte shift hydrogen evolution reaction on lead electrodes to more negative values. This can result in reduction of electrolyte decomposition and lower the self-discharge of battery [29].

The outcome of the undertaken research suggest, that ionic liquids presented in this study combined the properties originated from heteroatoms, long alkyl chain and sulfate ions which in consequence resulted in a good inhibition of corrosion process of lead alloy-calcium-tin alloy in sulfuric acid solution.

4. CONCLUSIONS

In the presented study ten new ionic liquids were tested in terms of corrosion inhibition properties as well as hydrogen and oxygen evolution reaction potential shift on lead-calcium-tin alloy submerged in sulfuric acid solution. Ionic liquids used in the experiments differed in terms of the anion and the length of alkyl substituent in cation. It was observed that corrosion parameters change after prolonged immersion time of the electrode in examined electrolyte. Experiments revealed that the best inhibition properties as well as the broadest electrochemical window can be achieved when hexadecyltrimethylammonium bisulfate is added as an electrolyte modifier. Ionic liquids with sulfate anion had a lower impact on those two parameters. This may be attributed to a less acidic character of

the anion. Corrosion current density decreased with increase of the side chain length up to sixteen carbon atoms. In the medium with longer substituent, this parameter started increasing again to higher values. This phenomenon was observed for both bisulfate and sulfate ionic liquids. Electrochemical impedance spectroscopy measurements showed that in thermodynamically stable conditions, after submerging electrode in electrolyte for five hours, adhesive layer of ionic liquid is formed on the surface of electrode. The thickest layer was observed for hexadecyltrimethylammonium bisulfate, which explains the best corrosion inhibition parameters of this specific electrolyte additive.

ACKNOWLEDGEMENTS

The authors would like to gratefully acknowledge the financial support from the National Centre of Research and Development of Poland, grant No PBS3/A5/43/2015, and Ministry of Science and Higher Education of Poland, grant No 03/31/DSPB/0356.

References

1. R. Yahmadi, K. Brik and F. Ben Ammar, *Int. J. Hydrogen Energy*, 42 (2017) 8765.
2. P. Lailier, F. Zaninotto, S. Nivet, L. Torcheux, J.-F. Sarrau, J.-P. Vaurijoux and D. Devilliers, *J. Power Sources*, 78 (1999) 204.
3. J. Lach and A. Czerwiński, *Int. J. Electrochem. Sci.*, 11 (2016) 9355.
4. J. Lach, S. Otrębowski and A. Czerwiński, *J. Electroanal. Chem.*, 742 (2015) 104.
5. H. Li, W.X. Guo, H.Y. Chen, D.E. Finlow, H.W. Zhou, C.L. Dou, G.M. Xiao, S.G. Peng, W.W. Wei and H. Wang, *J. Power Sources*, 191 (2009) 111.
6. W.R. Osório, L.C. Peixoto and A. Garcia, *J. Power Sources*, 238 (2013) 324.
7. W.R. Osório, L.C. Peixoto and A. Garcia, *Metall. Mater. Trans.*, A 46 (2016) 4255.
8. L.C. Peixoto, A.D. Bortolozzo, A. Garcia and W.R. Osório, *J. Mater. Eng. Perform.*, 25 (2016) 2211.
9. S. Pour-Ali, M.M. Aghili and A. Davoodi, *J. Alloys Compd.*, 652 (2015) 172.
10. G. Lin, G. Zhou, D. Li and M. Zheng, *J. Rare Earths*, 24 (2006) 232.
11. Y.-B. Zhou, C.-X. Yang, W.-F. Zhou and H.-T. Liu, *J. Alloys Compd.*, 365 (2004) 108111.
12. A. Li, Y. Chen, H. Chen, D. Shu, W. Li, H. Wang, C. Dou, W. Zhang and S. Chen, *J. Power Sources*, 189 (2009) 1204.
13. D.G. Li, J.D. Wang and D.R. Chen, *J. Power Sources*, 210 (2012) 163.
14. A.-R. El-Sayed, H.S. Mohran, H.M. Abd El-Lateef and H.A.S. Shilkamy, *J. Solid State Electrochem.*, 19 (2015) 1463.
15. A. Bhattacharya and I.N. Basumallick, *J. Power Sources*, 113 (2003) 382.
16. Z. Ghasemi and A. Tizpar, *Appl. Surf. Sci.*, 252 (2006) 3667.
17. M.A. Kiani, M.F. Mousavi, S. Ghasemi, M. Shamsipur and S.H. Kazemi, *Corros. Sci.*, 50 (2008) 1035.
18. C. Chiappe and D. Pieraccini, *J. Phys. Org. Chem.*, 19 (2005) 275.
19. B. Rezaei, E. Havakeshian and A.R. Hajipour, *J. Solid State Electrochem.*, 15 (2011) 421.
20. B. Rezaei, S. Mallakpour and M. Taki, *J. Power Sources*, 187 (2009) 605.
21. A. Gabryelczyk, K. Kopczyński, M. Baraniak, B. Łęgosz, F. Walkiewicz, J. Pernak, E. Jankowska, W. Majchrzycki, P. Kędzior and G. Lota, *J. Solid State Electrochem.*, 22 (2018) 919.
22. G. Lota, M. Baraniak, A. Gabryelczyk, K. Kopczyński, B. Łęgosz, J. Pernak, E. Jankowska, W. Majchrzycki and W. Rzesutek, *Przem. Chem.*, 96 (2017) 1208.
23. E. Gomez, N. Calvar and A. Dominguez, Thermal Behaviour of Pure Ionic Liquids, in: S. Handy (Eds.) *Ionic Liquids - Current State of the Art*, InTech, (2015) Rijeka, Croatia.
24. B. Rezaei, A.A. Ensafi and A.R.T. Jahromi, *Ionics*, 18 (2012) 109.

25. K. Kopczyński, A. Gabryelczyk, M. Baraniak, B. Łęgosz, J. Pernak, P. Kędzior and G. Lota, *Int. J. Electrochem. Sci.*, 13 (2018) 4390.
26. N. Sorour, C. Su, E. Ghali and G. Houlachi, *Electrochim. Acta*, 258 (2017) 631.
27. Z. Ghasemi and A. Tizpar, *Appl. Surf. Sci.*, 252 (2006) 3667.
28. A. Tizpar and Z. Ghasemi, *Appl. Surf. Sci.*, 252 (2006) 8630.
29. J. Yu, Z. Qian, M. Zhao, Y. Wang and L. Niu, *Chem. Res. Chin. Univ.*, 29 (2013) 374.

© 2018 The Authors. Published by ESG (www.electrochemsci.org). This article is an open access article distributed under the terms and conditions of the Creative Commons Attribution license (<http://creativecommons.org/licenses/by/4.0/>).